Advances in Materials Research, *Vol. 12, No. 4 (2023) 263-271*
https://doi.org/10.12989/amr.2023.12.4.263

Testing and evaluation of the corrosion behavior of Aluminum/Alumina bulk composites fabricated via combined stir casting and APB process

Abdalkareem Jasim[1], Ghassan Fadhil Smaisim[*2,3], Abduladheem Turki Jalil[4,5], Surendar Aravindhan[6], Abdullah Hasan Jabbar[7], Shaymaa Abed Hussein[8], Muneam Hussein Ali[9], Muataz S. Alhassan[10] and Yasser Fakri Mustafa[11]

[1]*Al-maarif University College, Medical Laboratory Techniques Department, Al-anbar-Ramadi, Iraq*
[2]*Department of Mechanical Engineering, Faculty of Engineering, University of Kufa, Iraq*
[3]*Nanotechnology and Advanced Materials Research Unit, Faculty of Engineering, University of Kufa, Iraq*
[4]*Faculty of Biology and Ecology, Yanka Kupala State University of Grodno, 230023 Grodno, Belarus*
[5]*College of Technical Engineering, The Islamic University, Najaf, Iraq*
[6]*Department of Pharmacology, Saveetha Dental College and Hospital, Saveetha Institute of Medical and Technical Sciences, Chennai, India*
[7]*Optical Department, College of Medical and Health Technology, Sawa University, Ministry of Higher Education and Scientific Research, Al-Muthanaa, Samawah, Iraq*
[8]*Al-Manara College for Medical Sciences, Maysan, Iraq*
[9]*Al-Nisour University College, Baghdad, Iraq*
[10]*Division of Advanced Nano Material Technologies, Scientific Research Center, Al-Ayen University, Thi-Qar, Iraq*
[11]*Department of Pharmaceutical Chemistry, College of Pharmacy, University of Mosul, Mosul-41001, Iraq*

(Received January 22, 2022, Revised May 10, 2022, Accepted August 18, 2022)

Abstract. In this study, AA1060/Alumina composites were fabricated by combined stir casting and accumulative press bonding (APB). The APB process was repeated up to six press bonding steps at 300Ċ. As the novelty, potential dynamic polarization in 3.5Wt% NaCl solution was used to study the corrosion properties of these composites. The corrosion behavior of these samples was compared and studied with that of the annealed aluminum alloy 1060 and versus the number of APB steps. So, as a result of enhancing influence on the number of APB process, this experimental investigation showed a significant enhancement in the main electrochemical parameters and the inert character of the Alumina particles. Together with Reducing the active zones of the material surfaces could delay the corrosion process. Also, at higher number of steps, the corrosion resistance of composites improved. The sample produced after six number of steps had a low corrosion density in comparison with high corrosion density of annealed specimens. Also, the scanning electron microscopy (SEM), was used to study the corrosion surface of samples.

Keywords: accumulative press bonding (APB); corrosion; pitting corrosion; polarization

∗Corresponding author, Associate Professor, E-mail: Ghassan.Smaisim@uokufa.edu.iq

http://www.techno-press.org/?journal=amr&subpage=5 ISSN: 2234-0912 (Print), 2234-179X (Online)

1. Introduction

As a new group of advanced materials, aluminum based composites are being considered in several industries especially such as automobile and aerospace due to their desirable properties such as being light having high strength and coefficient of thermal expansion and so on (Vini *et al.* 2017, Farhadipour *et al.* 2018, Heydari Vini *et al.* 2020). Severe plastic deformation (SPD) processes are now widely used to produce ultrafine-grained (UFG) materials (Seah *et al.* 2003, Supat *et al.* 2021). These processes are such as accumulative roll bonding (Sedighi *et al.* 2016), accumulative press bonding (Amirkhanlou *et al.* 2014), multi-axial forging (Lee and Kang 2011), cyclic extrusion compression (CEC) (Chen *et al.* 2008) and so on. During APB, pressing is done on cumulated bars with same dimensions. Usually, the thickness reduction per each step of pressing is 50% and two bars are bonded together during the pressing process. This process is capable to achieve a composite via cumulative pressing without any change in their dimensions by inserting extra plastic strains on them including cutting, surface degreasing with acetone, brushing and stacking together for the next press bonding step (Vini and Daneshmand 2019, 2020). During the recent years, mechanical properties, texture and microstructure evolution of SPD processed metals and alloys have been the topic of many researches (Borhani 2016, Sereshki *et al.* 2016). Also, many investigations have been done on the effect of additive particles on the oxidation and corrosion of composite materials (Tjahjono *et al.* 2021, Bakhtadze *et al.* 2020, Mikhailov and Chachkov 2020, Kianfar 2019). However, the corrosion behavior of these APB-processed samples needs an in depth investigation. Many researchers investigated the corrosion behavior of aluminum based composite samples fabricated by SPD techniques such as ARB and showed the effect of its parameters on the properties of the MMCs (Darmiani *et al.* 2013, Wang *et al.* 2022, Gao *et al.* 2022). In the present study and as the novelty, a 3.5Wt-% NaCl aqueous solution at room temperature was used to analyze the corrosion behavior of Al/alumina composites fabricated at 300°C for the first time. To stabilize the open-circuit potential (E_{corr}) with a 50 mv min^{-1} of sweeping rate, the samples were immersed into the electrolyte for about 30 min. In all potentio dynamic tests. Intersection of the cathodic and anodic Tafel curves extrapolated from the anodic and cathodic polarization curves were used to study the values of the corrosion potential (E_{corr}) and the corrosion current density (I_{corr}) (Mikhailov and Chachkov 2020, Kianfar 2019, Darmiani *et al.* 2013, Vini *et al.* Reihanian *et al.* 2013, Vini *et al.* 2017).

2. Experimental procedure

2.1 The stir casting process

The fully annealed alloy 1060 is used as raw material aluminum. Alumina particles as additive particles with average grain size 2 micrometers are used as reinforcement with purity 99%. Before the casting process, the additive particles were preheated at 400Ċ for 5 hours to diminish their humidity. The alumina particles with Wt. 5% were put on the surface of the aluminum melt at 750Ċ and this composition was rotated with a rotary speed of 650 rpm with the blowing of Argon gas to protect the melt from oxidation. The stir casting process allows to create a desirable bonding between aluminum and alumina particles which leads to decreasing the amount of voids and cavities in the final composite matrix. The dimension of the final fabricated composite samples is 200×15×5 mm. Brushing the surface of composite samples prior, the APB process in necessary to

Table 1 The APB process steps for fabrication of Al/ alumina composites

No. of steps	Pressing temperature (°C)	No. of composite layers	Reduction in steps (%)	Composite layer thickness (μm)	Final reduction (%)	Plastic strain
1	300	2	50	5000	50	0.8
2	300	4	50	2500	75	1.6
3	300	8	50	1250	87.5	2.4
4	300	16	50	625	93.75	3.2
5	300	32	50	312.5	96.87	4
6	300	64	50	156.25	98.43	4.8

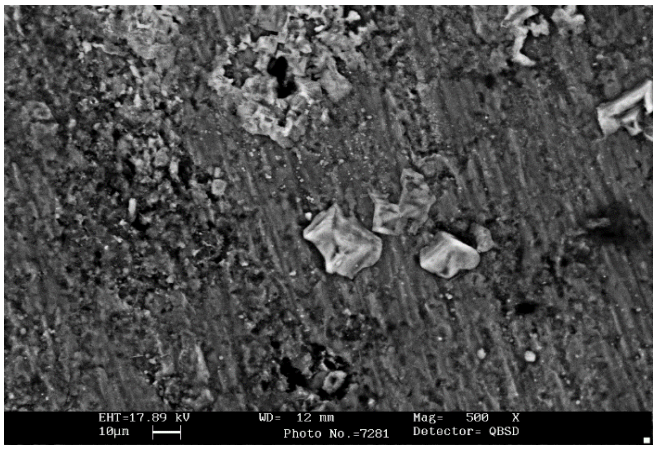

Fig. 1 SEM micrographs of Al/ Alumina composites after three APB steps

create a desirable bonding. As mentioned before, brushing allows to deliver a coarse surface which increases the introduces a restricted shear during the forming process which disrupts the oxide layers. This disruption creates more cracks and allows the virgin metals to extrude along the cracks and toward the opposite composite layers which create metallic bonding (Vini and Daneshmand 2019).

2.2 The APB process

At the starting of the next stage to set up the APB process and to clean the illuminations and grease from the surface of the composite samples, the samples were putted in the acetone bath for 30 minutes. Then, two bars put on together preheated at 300Ċ for 10 minutes (preheating) and were pressed (50% reduction in thickness). Then, this process was repeated up to six steps. The APB process was continued up to six steps with 5 Wt.% of alumina particles. The APB steps of the process are summarizing in Table 1.

A 3.5 Wt. % NaCl aqueous solution on the 1 cm^2 of samples at the room temperature was used for doing the corrosion tests. To stabilize the open-circuit potential, the samples were deep into the electrolyte for about 30 min. For all potentio dynamic tests, the sweeping rate was 1 mV. min^{-1}. The intersection of the cathodic and anodic Tafel curves extrapolated from the anodic and cathodic polarization curves were used to calculate the values of the corrosion potential (E_{corr}) and the corrosion current density (I_{corr}).

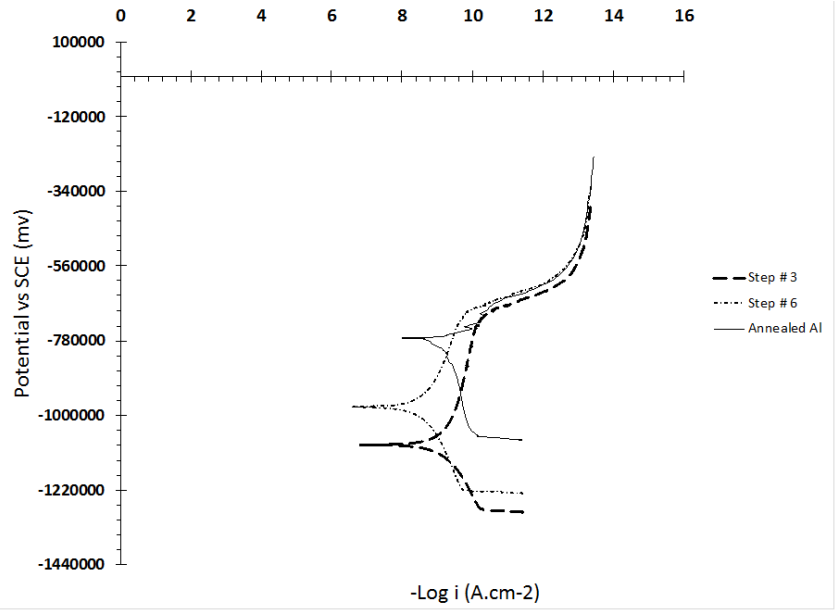

Fig. 2 Potentiodynamic polarization curves and its anodic part of the annealed Al and APB processed composites

3. Results and discussion

Fig. 1 shows the microstructure of the composites cross section in step #3. According to Fig. 1, during the APB process, the size and thickness of dense clusters decreases accordingly. Fig. 1 shows that the uniformity of clusters increases after the 3th step, significantly. The Al matrix flows among the particles where dispersed uniformly through the Al matrix during the forming process.

For sample with three and six number of steps, the potentio dynamic polarization curves recorded are shown in Fig. 2. Also, the polarization diagrams for these samples are given in Table 2. Formation of a non- protective passive layer for the surface of all samples leads to showing an active behavior in the anodic potential. In general, Al has a permanent oxide film on its surface because of the reaction between Al and atmosphere oxygen. So, due to the senility of Al to pitting corrosion in aqueous media, it is dangerous for formation of the protective passive film. At higher corrosion current densities, the anodic potential of the produced samples is more positive than annealed Al (Chen *et al.* 2021, Darmiani *et al.* 2013). Table 2 shows the lowest corrosion current density for the six step APB processed sample. According to Table 2, β_a, β_c, E_{corr}, I_{corr}, R_p and V_{corr} are the slope of the anodic and cathodic curves, corrosion resistance, the density of corrosion current, polarization resistance and the corrosion sped of samples, respectively.

Moreover, the kinetics of material corrosion whereas the corrosion current density, I_{corr} and the corrosion potential, E_{corr}, represents a thermodynamic characteristic of a given metal-electrolyte system means the corrosion value more precisely. These results indicate that in comparison with the pure Al, the corrosion resistance of the sample with three steps can be improved. It means that increasing the number of steps leads to increasing the corrosion potential which is due to the decreasing the activity of the sample surfaces (Mikhailov and Chachkov 2020, Reihanian *et al.* 2013, Korchef and Kahoul 2013). Fig. 3 shows the Stern- Geary corrosion polarization resistance

Table 2 The potentio dynamic polarization values recorded for samples

Sample	β_c (mV/decade)	β_a (mV/decade)	E_{corr} (V vs. SCE)	I_{corr} (μA/cm^2)	R_p (KΩ.cm^2)	V_{corr} (μm/year)
Step #3	128	299	-1.1	0.24	164	13.22
Step #6	169	215	-0.98	0.06	661	7.18
Annealed Al	292	71	-0.78	0.3	85	16.16

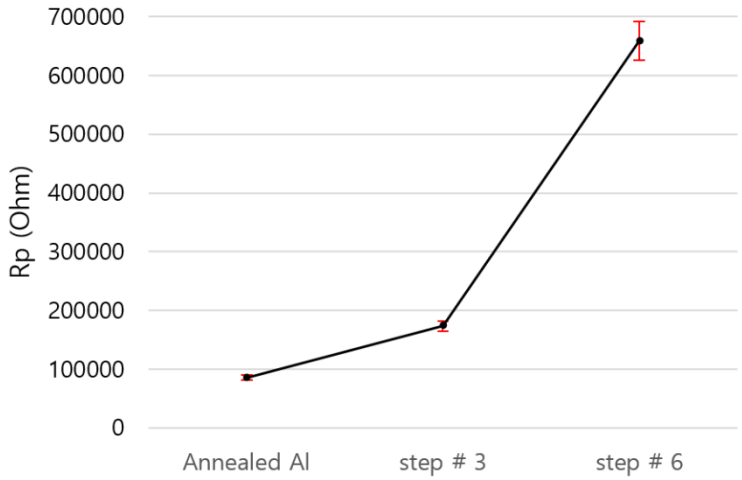

Fig. 3 Effect of steps on the corrosion polarization resistance (Rp) of composites

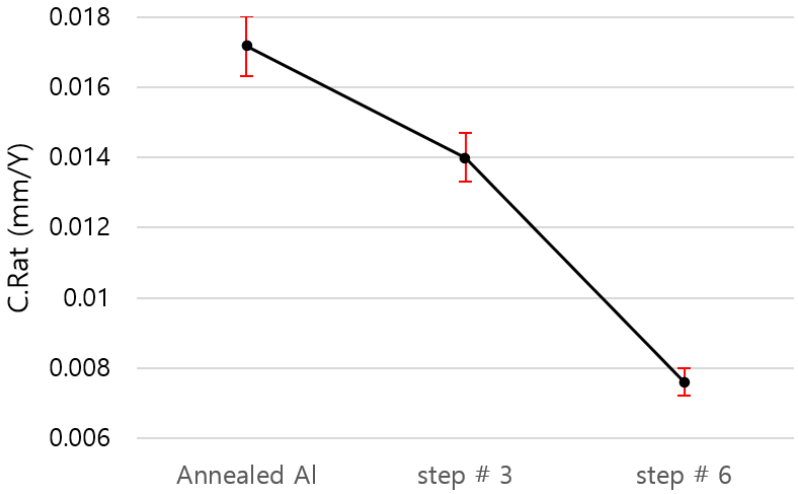

Fig. 4 Effect of steps No. on the corrosion speed of composites

(R_p) of samples versus the number of APB steps. Fig. 3 shows that the sample produced with six steps has the most corrosion polarization resistance while the annealed Al has the lowest value. This value for the sample with six steps is about six times more than that of the annealed Al.

Fig. 4 shows the corrosion speed (R_p) of samples versus the number of APB steps. According to Fig. 4, sample produced with three steps has the most corrosion speed while the annealed Al has

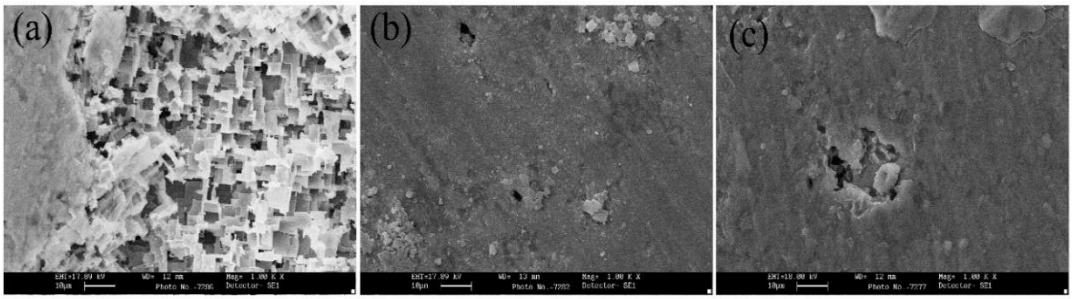

Fig. 5 SEM micrographs of APB processed samples after electrochemical tests in two magnifications (a) Annealed Al and after, (b) 3 and (c) 6 steps of APB process

the lowest value. So, Alumina particles has a significant effect on the structural refinement by increasing the number of APB steps. Two mechanisms (dislocation strengthening and grain boundary strengthening mechanism) can explain the strengthening of the Al matrix during the APB process. Vini and Daneshmand (2019, 2022) at lower number of steps especially No.2, the work hardening of the aluminum matrix has a main role for increasing the strength.

In the Al/Alumina composites, the non-deformable Alumina particles stimulate slip systems of metallic matrix near its adjacent layers and therefore, the density of dislocations and the strain hardening rise from the first step up to the 6^{th}. The plastic flow between the clusters creates uniform distribution of the reinforcement at higher steps and as a result, the distance between the particles increases. In the other words, it is clear that the regions with high density of dislocations have different electrochemical behavior in comparison with the regions made of coarse grains and low density of dislocations. So, decreasing the grain size leads to decreasing the rate of corrosion, Fig. 4.

Al and its alloys become hydrated when are in touch with a watery solution and produce a hydrated oxide film (AlOOH which is considerable as Al_2O_3. H_2) on their surfaces. The production of the hydrated oxide is

$$Al + H_2O \rightarrow AlOH + H^+ + e^- \quad (1)$$

$$AlOH + H_2O \rightarrow Al(OH)_2 + H^+ + e^- \quad (2)$$

$$AlOOH + H^+ + e^- \rightarrow Al(OH)_2 \quad (3)$$

So, the main reaction is

$$Al + 2H_2O \rightarrow AlOOH + 3H^+ + 3e^- \quad (4)$$

Increasing the strengthening mechanism during the APB process, raises the chemical activity of surface. This is steady with the higher cathodic polarization current density of the sample fabricated with six steps which shows the higher reduction rate of H+ ions to H_2 atoms. During the corrosion, both of the reduction reactions and oxidation should be considered in the equilibrium condition **(**Darmiani *et al.* 2013, Reihanian *et al.* 2013, Reihanian *et al.* 2013)

The APB processed samples have the ability to form an oxide layer with the lowest cathodic reaction rate. So, the anodic potential of samples is nobler than that of the annealed Al with the lowest cathodic current density due to the presence of alumina particles. These particles shift the equilibrium condition of the corrosion process to the lower value of I_{corr} due to the activity of the surface and the cathodic reaction and can improve the corrosion resistance (Reihanian *et al.* 2013,

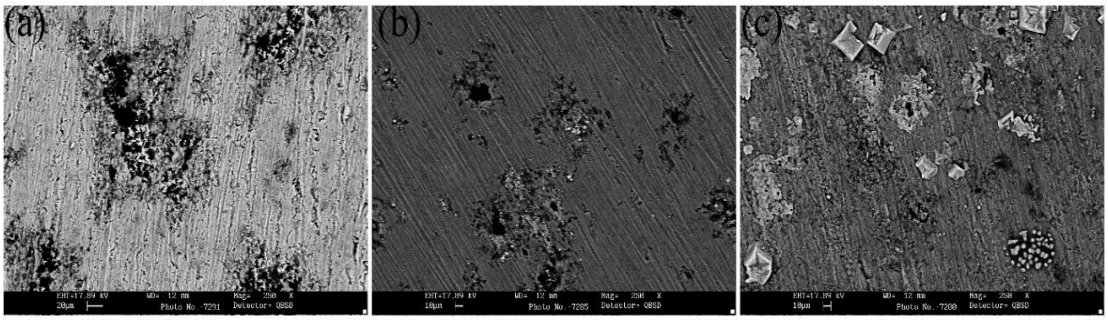

Fig. 6 SEM micrograph of pits propagated in the Al matrix (a) Annealed Al and after, (b) three and (c) six steps of APB process

Korchef and Kahoul 2013). Fig. 5 shows the SEM micrographs of all specimens. As shown in Fig. 5, by increasing the number of APB steps, the number of pits increases and their depth decreases, the uniformity of their distribution decreases and their length increase which leads to generation of longer pits.

Fig. 6 shows the localized corrosion zones and cracks on the surface of samples. As can be seen in Fig. 6, the beginning of the local corrosion process is near the alumina particles (secondary phase) or grain boundaries. Materials with high amounts of dislocations and grains boundary density, equilibrates the energy in all parts and facilitates the generation of surface layer. So, due to the high amounts of the energy trapped in the un-equilibrated grain boundaries during the APB process, the generation of the surface layer for the UFG materials energy equilibrium for the un-equilibrated grain boundaries and grain boundary defects leads to a uniform and more homogeneous corrosion. In the other words, severe plastic deformation of the pressing process, increasing the density of dislocations and creation an ultra-fine grain structure are the most important factors for improvement of the corrosion resistance of aluminum alloy 1060.

4. Conclusions

1) After three APB steps, a uniform distribution of particles through the matrix is achieved.
2) Increase in the strain energy of the material due to the formation of fine grains, decreases the corrosion resistance of Al and increases the cathodic reaction during the APB. These variation of results during the experimental tests are due to lack of filtering of results obtained.
3) The composite sample with six number of APB steps has the lowest corrosion current density and the highest charge transfer resistance. This behavior decreases the cathodic reaction rate of the hybrid composite that causes the chemical activity of the surface and is due to the inert effect of the particles.
4) By increasing the number of APB steps, the number and length of theses pits increased and their depth decreased too.

References

Amirkhanlou, S., Ketabchi, M., Parvin, N., Khorsand, S. and Carreño, F. (2014), "Manufacturing of

nanostructured Al/WCp metal- matrix composites by accumulative press bonding", *IOP Conf. Ser.: Mater. Sci. Eng.*, **63**(1), 012001. https://doi.org/10.1088/1757-899X/63/1/012001.

Bakhtadze, V., Mosidze, V., Machaladze, T., Kharabadze, N., Lochoshvili, D., Pajishvili, M. and Mdivani, N. (2020), "Activity of Pd-MnOx/Cordierite (Mg, Fe) 2Al4Si5O18) catalyst for carbon monoxide oxidation", *Eur. Chem. Bull.*, **9**(2), 75-77.

Chen, H., Dmitry, B., Supat, C., Maboud, H., Mahmoud, M.Z., Sabetvand, R., Duan, J. and Toghraie, D. (2021), "Combustion process of nanofluids consisting of oxygen molecules and aluminum nanoparticles in a copper nanochannel using molecular dynamics simulation", *Case Stud. Therm. Eng.*, **28**, 101628. https://doi.org/10.1016/j.csite.2021.101628.

Chen, Y.J., Wang, Q., Roven, H.J., Liu, M.P., Karlsen, M., Yu, Y.D. and Hjelen, J. (2008), "Network-shaped fine- grained microstructure and high ductility of magnesium alloy fabricated by cyclic extrusion compression", *Scripta Mater.*, **58**(4), 311-314. https://doi.org/10.1016/j.scriptamat.2007.09.058.

Darmiani, E., Danaee, I., Golozar, M.A. and Toroghinejad, M.R. (2013), "Corrosion investigation of Al-SiC Nano-composite fabricated by accumulative roll bonding (APB) process", *J. Alloy. Compound.*, **552**, 31-39. https://doi.org/10.1016/j.jallcom.2012.10.069.

Farhadipour, P., Sedighi, M. and Heydari Vini, M. (2018), "Influence of temperature of accumulative roll bonding on the mechanical properties of AA5083/1% Al_2O_3 composite", *Powder Metallurg. Metal Ceram.*, **56**(9-10), 496-503. https://doi.org/10.1007/s11106-018-9921-0.

Gao, Y., Vini, M.H. and Daneshmand, S. (2022), "Effect of nano Al_2O_3 particles on the mechanical and wear properties of Al/Al_2O_3 composites manufactured via ARB", *Rev. Adv. Mater. Sci.*, **61**(1), 734-743. https://doi.org/10.1515/rams-2022-0268.

Heydari Vini, M. and Daneshmand S. (2020), "Fabrication of bimetal aluminum-5% alumina-bromine composites by warm accumulative roll bonding", *J. Test. Eval.*, **49**(4), 2757-2766.

Heydari Vini, M. and Sedighi, M. (2017)., "Mechanical properties and bond strength of bimetallic AA1050/AA5083 laminates fabricated by warm-accumulative roll bonding", *Can. Metal. Quart.*, **45**, 160-167. https://doi.org/10.1080/00084433.2017.1405539.

Heydari Vini, M., Sedighi, M. and Mondali, M. (2017), "Investigation of bonding behavior of AA1050/AA5083 bimetallic laminates by roll bonding technique", *Trans. Ind. Inst. Metal.*, **71**(9), 2089-2094. https://doi.org/10.1007/s12666-017-1058-1.

Kianfar, F. and Kianfar, E. (2019), "Synthesis of isophthalic Acid/aluminum nitrate thin film nanocomposite membrane for hard water softening", *J. Inorg. Organomet. Polym.*, **29**, 2176-2185. https://doi.org/10.1007/s10904-019-01177-1.

Korchef, A. and Kahoul, A. (2013), "Corrosion behavior of commercial aluminum alloy processed by equal channel angular pressing", *J. Corros.*, **2013**, Article ID 983261. https://doi.org/10.1155/2013/983261.

Lee, S.M. and Kang, C. (2011), "Effect of solid fraction on formability and mechanical properties in a vertical-type rheo squeeze-casting process", *Proc. Inst. Mech. Eng. Part B, J. Eng. Manuf.*, **225**(B2), 184-196. https://doi.org/10.1243/09544054JEM1874.

Mikhailov, O.V. and Chachkov, D.V. (2020), "Molecular structure models of Al2Ti3 and Al2V3 clusters according to DFT quantum-chemical calculations", *Eur. Chem. Bull.*, **9**(2), 62-68.

Reihanian, M., Lari Baghal, S.M., Keshavarz Haddadian, F. and Paydar, M.H. (2016). "A comparative corrosion study of Al/Al2O3-SiC hybrid composite fabricated by Accumulative Roll Bonding (ARB)", *J. Ultraf. Grain. Nanostr. Mater.*, **49**(1), 29-35. https://doi.org/10.7508/jufgnsm.2016.01.05.

Seah, K.H.W., Hemanth, J. and Sharma, S.C. (2003), "Effect of high-rate heat transfer during casting on the strength, hardness and wear behavior of aluminum-quartz particulate metal matrix composites", *Proc. Inst. Mech. Eng. Part B*, *J. Eng. Manuf.*, **217**(5), 651-659.

Sedighi, M., Vini, M.H. and Farhadipour, P. (2016), "Effect of alumina content on the mechanical properties of AA5083/Al2O3 composites fabricated by warm accumulative roll bonding", *Powder Metallurg. Metal Ceram.*, **55**(7), 413-418. https://doi.org/10.1007/s11106-016-9821-0.

Sereshki, M., Azad, B. and Borhani, E. (2016), "Corrosion behavior of Al-2wt%Cu alloy processed by Accumulative Roll Bonding (APB) process", *J. Ultraf. Grain. Nanostr. Mater.*, **49**(1), 22-28. https://doi.org/10.7508/jufgnsm.2016.01.04.

Supat, C., Olegovich Bokov, D., Suksatan, W., Landowski, M., Fydrych, D., Abdullah, M.E. and Aghajani Derazkola, H. (2021), "Pin angle thermal effects on friction stir welding of AA5058 aluminum alloy: CFD simulation and experimental validation", *Mater.*, **14**(24), 7565. https://doi.org/10.3390/ma14247565.

Tjahjono, T., Elveny, M., Chupradit, S., Bokov, D., Hoi, H.T. and Pandey, M. (2021), "Role of cryogenic cycling rejuvenation on flow behavior of ZrCuAlNiAg metallic glass at relaxation temperature", *Trans. Ind. Inst. Metal.*, **74**(12), 3241-3247. https://doi.org/10.1007/s12666-021-02395-3.

Vini, M.H. and Daneshmand, S. (2020), "Corrosion of Al/TiO2 composites fabricated by accumulative roll bonding", *Mater. Perform.*, **59**(11), 28-31.

Vini, M.H. and Daneshmand, S. (2019), "Bonding evolution of bimetallic Al/Cu laminates fabricated by asymmetric roll bonding", *Adv. Mater. Res.*, **8**(1), 1-10. https://doi.org/10.12989/amr.2019.8.1.001.

Vini, M.H. and Daneshmand, S. (2019), "Investigation of bonding properties of Al/Cu bimetallic laminates fabricated by the asymmetric roll bonding techniques", *Adv. Comput. Des.*, **4**(1), 33-41. https://doi.org/10.12989/acd.2019.4.1.033.

Vini, M.H. and Daneshmand, S. (2022), "Mechanical and wear properties evaluation of Al/Al2O3 composites fabricated by combined compo-casting and WARB process", *Adv. Comput. Des.*, **7**(2), 129-137. https://doi.org/10.12989/acd.2022.7.2.129.

Wang, W., Vini, M.H. and Daneshmand, S. (2022), "Mechanical and wear properties of Al/tic composites fabricated via combined compo-casting and APB process", *Crystal.*, **12**(10), 1440. https://doi.org/10.3390/cryst12101440.

CC